Structural Variation in Manganase Complexes: Synthesis and Characterization of Manganese Complexes from Carboxylate-containing Chelating Ligands

Hitoshi Iikura[1a] and Toshi Nagata*,[1a,b]

Department of Chemistry, Graduate School of Science, Kyoto University, Kyoto 606-8502, Japan, and Institute for Molecular Science, Myodaiji, Okazaki 444-8585, Japan

Three manganese(II) complexes, $[Mn^{II}_2L^1_2(H_2O)_4](ClO_4)_2 \cdot H_2O$ (**1**, L^1H = (bis(2-pyridylmethyl)amino)acetic acid), $[Mn^{II}_2L^2_2(H_2O)_2](BPh_4)_2 \cdot 2EtOH \cdot 2H_2O$ (**2**, L^2H = 3-(bis(2-pyridylmethyl)amino)propionic acid), $\{[Mn^{II}_2L^2_2(H_2O)-(MeCN)](BPh_4)_2 \cdot 2MeCN\}_\infty$ (**3**), and a manganese(IV) complex $[Mn^{IV}_2O_2L^2_2](ClO_4)_2 \cdot 4H_2O$ (**4**) were synthesized and characterized by X-ray crystallography. The compound **1** was a dinuclear Mn^{II}_2 complex which crystallized in the monoclinic crystal system, space group $P2_1/n$, with $Z = 4$, $a = 12.19(1)$ Å, $b = 14.623(8)$ Å, $c = 21.72(1)$ Å, $\beta = 96.29(6)°$, $V = 3849(4)$ Å^3. The complex cation had an approximate C_2 symmtery. The two manganeses were both seven-coordinate and doubly bridged by one oxygen atom of carboxylate groups in μ_2,η^1-mode. The compound **2** was also a dinuclear Mn^{II}_2 complex which crystallized in the monoclinic crystal system, space group $P2_1/n$, with $Z = 2$, $a = 16.760(2)$ Å, $b = 9.643(2)$ Å, $c = 23.533(2)$ Å, $\beta = 92.984(8)°$, $V = 3798.4(7)$ Å^3. The complex cation of **2** also had two seven-coordinate manganese ions, but unlike **1** the nonbridging carboxylate oxygens weakly coordinate to the manganese ions. The compound **3** crystallized in the orthorhombic crystal system, space group $P2_12_12_1$, with $Z = 4$, $a = 27.888(3)$ Å, $b = 29.054(2)$ Å, $c = 9.428(2)$ Å, $V = 7638(2)$ Å^3. The cationic portion of **3** consisted of infinite chains of Mn^{II} (two Mn^{II} ions per an asymmetric unit) bridged by carboxylates in bidentate syn/anti mode. The compound **4** was a dinuclear bis(μ-oxo) Mn^{IV}_2 complex which crystallized in the trigonal crystal system, space group $R\bar{3}$, with $Z = 8$, $a = 23.962(4)$ Å, $c = 17.190(3)$ Å, $V = 8547(3)$ Å^3. All these structures are made up from a common fragment "L^nMn" assembling in various topologies. Variable-temperature magnetic susceptibility measurements revealed that the Mn^{II} ions in **1**−**3** were weakly antiferromagnetically coupled ($J = -0.631(6)$, $-0.655(5)$, and $-0.20(1)$ cm^{-1} for **1**−**3**), and that the Mn^{IV} ions in **4** were strongly antiferromagnetically coupled ($J = -97.5(5)$ cm^{-1}). The cyclic voltammogram of **4** showed two reduction waves with $E_{1/2}$ values of -0.52 and 0.28 V (vs ferrocene). These $E_{1/2}$ values are more negative by 0.1 V than those of the closely related complex $[Mn^{III}Mn^{IV}O_2L^1_2](ClO_4)$.

During the past two decades, considerable efforts have been focused on the synthesis and characterization of polynuclear manganese complexes.[2] Many of these studies are directed toward the preparation of synthetic models for the various manganese enzymes such as manganese catalase and photosynthetic water oxidase.[3] These synthetic complexes employ various donor groups,[2] among which the carboxylate donor group is particularly important because of its biological relevance,[4] although other donor groups have also been successfully utilized in model compounds.

Manganese complexes containing carboxylate ligands have been extensively studied. These studies have revealed the rich structural (as well as chemical and magnetochemical) diversity of manganese carboxylates, with various nuclearity (Mn_1 to Mn_{18}) and various binding modes of carboxylates (syn/anti, monodentate/bidentate, bridging/terminal). Most of the multinuclear clusters are formed by "self-assembly" reactions,[5] often employing additional ligands (mononucleating[6] or binucleating[7]) or polycarboxylate anions,[8] while Hendrickson and Christou have developed transformation of preformed clusters by use of electrophilic reagents.[9] Both of these methods have proven useful for preparation of manganese carboxylate clusters; however, it is very difficult to construct particular structures *by design* starting from simple carboxylates such as acetate or benzoate, because of the stunning number of possible structural arrangements for even a small number of manganese and carboxylate ions.

A potentially useful approach to overcome such difficulty is to introduce a carboxylate group within a polydentate chelating ligand, in a similar manner as in EDTA (ethylenediaminetetraacetic acid).[10a] There are, however, reported only a few

(1) (a) Kyoto University. (b) Institute for Molecular Science.

(2) Wieghardt, K. *Angew. Chem., Int. Ed. Engl.* **1989**, *28*, 1153.

(3) (a) *Manganese Redox Enzymes*; Pecoraro, V. L., Ed.; VCH: New York, 1992. (b) Dismukes, G. C. *Chem. Rev.* **1996**, *96*, 2909. (c) Yachandra, V. K.; Sauer, K.; Klein, M. P. *Chem. Rev.* **1996**, *96*, 2927.

(4) (a) Christou, G. *Acc. Chem. Res.* **1989**, *22*, 328. (b) Que, L., Jr.; True, A. E. *Prog. Inorg. Chem.* **1990**, *38*, 97. (c) Lardin, R. L.; Tolman, W. B.; Lippard, S. J. *New J. Chem.* **1991**, *15*, 417. (d) Some of the manganese enzymes have the carboxylate-bridged binuclear manganese active sites.[3b] It has been proposed that the photosynthetic water oxidase also has the ligating carboxylate groups from the protein side chains.[4e,f] (e) Tamura, N.; Ikeuchi, M.; Inoue, Y. *Biochim. Biophys. Acta* **1989**, *973*, 281. (f) Andreasson, L.-E. *Biochim. Biophys. Acta* **1989**, *973*, 465.

(5) (a) Karipides, A.; Reed, A. T. *Inorg. Chem.* **1976**, *15*, 44. (b) Kennard, C. H.; Smith, G.; O'Reilly, E. J.; Chiangjin, W. *Inorg. Chim. Acta* **1983**, *69*, 53. (c) Ardiwinata, E. S.; Craig, D. C.; Phillips, D. J. *Inorg. Chim. Acta* **1989**, *166*, 233. (d) Devereux, M.; McCann, M.; Casey, M. T.; Curran, M.; Ferguson, G.; Cardin, C.; Convery, M.; Quillet, V. *J. Chem. Soc., Dalton Trans.* **1995**, 771. (e) Wemple, M. W.; Tsai, H.-L.; Wang, S.; Claude, J. P.; Streib, W. E.; Huffman, J. C.; Hendrickson, D. N.; Christou, G. *Inorg. Chem.* **1996**, *35*, 6437. (f) Tangoulis, V.; Psomas, G.; Dendrinou-Samara, C.; Raptopoulou, C. P.; Terzis, A.; Kessissoglou, D. P. *Inorg. Chem.* **1996**, *35*, 7655.

structurally characterized manganese complexes with carboxylate-containing polydentate chelating ligands.[10] Among the promising carboxylate-containing ligands are anions of bis(2-pyridylmethyl)aminoacetic acid (L^1H)[10c,11,12] and 3-(bis(2-pyridylmethyl)amino)propionic acid (L^2H).[13a] The ligand L^1 was utilized by Suzuki et al. to prepare a mixed-valence Mn^{III}-Mn^{IV} complex,[10c] while the manganese complex of the ligand L^2, first described by McKenzie and co-workers,[13a] has been characterized only by electrospray mass spectrometry.[13b]

We report here the syntheses and characterization of four new manganese complexes derived from L^1 and L^2. Complex **1**, $[Mn^{II}_2L^1_2(H_2O)_4](ClO_4)_2 \cdot H_2O$, is an Mn^{II}_2 complex which has a totally different structure from Suzuki's $Mn^{III}Mn^{IV}$ complex;[10c]

complex **2**, $[Mn^{II}_2L^2_2(H_2O)_2](BPh_4)_2 \cdot (EtOH)_2 \cdot 2H_2O$, is an Mn^{II}_2 complex of L^2 with a similar structure as **1**; complex **3**, $\{[Mn^{II}_2L^2_2(H_2O)(MeCN)](BPh_4)_2 \cdot 2MeCN\}_\infty$, is also an Mn^{II} complex of L^2 but with a polymeric structure; and complex **4**, $[Mn^{IV}_2O_2L^2_2](ClO_4)_2 \cdot 4H_2O$, is an Mn^{IV}_2 complex with an $Mn(\mu\text{-}O)_2Mn$ core. Despite the apparent structural variation, all complexes share a common fragment "L^nMn", and the differences in the structures can be ascribed to the different concatenation topology of the fragments.

Experimental Section

General. The following reagents were used as received: 2-chloromethylpyridine hydrochloride, NaBPh$_4$ (Tokyo Kasei); glycine, 3-aminopropionic acid, Mn(NO$_3$)$_2$·6H$_2$O, NaClO$_4$, 30% H$_2$O$_2$ (Nacalai Tesque); Mn(ClO$_4$)$_2$·6H$_2$O (Alfa). Water was purified by an Advantec GS-20A apparatus (distillation after passing through an ion-exchange resin). ^{1}H NMR spectra were recorded on JEOL GX-400 and Alpha-500 spectrometers. Elemental analyses were performed at the Microanalysis Center of Kyoto University.

Caution! *Organic perchlorate salts are potentially explosive. Although we have experienced no accidents so far, all compounds containing perchlorate should be handled with care and in small amounts.*

Ligand Synthesis. (Bis(2-pyridylmethyl)amino)acetic Acid (L^1H). The following procedure is based on Suzuki's report[10c] with a slight modification. 2-Chloromethylpyridine hydrochloride (6.0 g, 37 mmol) and glycine (1.38 g, 18.4 mmol) were dissolved in water (20 mL) and stirred at room temperature for 5 days, with addition of 5 mol dm^{-3} aqueous NaOH solution at intervals to maintain the pH at 8−10. The resulting dark red solution was extracted with CHCl$_3$, and then the aqueous phase was acidified to pH 3−4 by 1 mol dm^{-3} HCl and extracted again with CHCl$_3$. The aqueous phase was neutralized (pH 7) by aqueous NaOH and evaporated. The residue was dissolved in 2-propanol, and the insoluble solid (NaCl) was filtered. Pale-yellow crystals of L^1H formed from the filtrate, which were collected and dried under vacuum. Yield: 1.9 g (7.2 mmol, 40%). ^{1}H NMR (CDCl$_3$): 3.62 (s, 2H, CH$_2$), 4.08 (s, 4H, PyCH$_2$), 7.23, 7.66 (each t, 2H, PyH), 7.26, 8.57 (each d, 2H, PyH). Anal. Found: C, 64.99; H, 5.79; N, 16.35; O, 12.67. Calcd: C, 65.36; H, 5.88; N, 16.33; O, 12.44.

3-(Bis(2-pyridylmethyl)amino)propionic Acid (L^2H). This compound was synthesized by a similar procedure as in L^1H, except that 3-aminopropionic acid was used instead of glycine. Starting from 2.97 g (18.1 mmol) of 2-chloromethylpyridine, 0.81 g (9.5 mmol) of 3-aminopropionic acid, pale-red crystals of L^2H were obtained. Yield: 1.1 g (3.9 mmol, 42%). ^{1}H NMR (CDCl$_3$): 2.62, 3.02 (each t, 2H, CH$_2$), 3.94 (s, 4H, PyCH$_2$), 7.20, 7.64 (each t, 2H, PyH), 7.32, 8.56 (each d, 2H, PyH). Anal. Found: C, 66.04; H, 6.26; N, 15.47. Calcd: C, 66.40; H, 6.32; N, 15.49. The ^{1}H NMR of this product was consistent with the reported spectrum.[13a]

Complex Synthesis. $[Mn^{II}_2L^1_2(H_2O)_4](ClO_4)_2 \cdot H_2O$, 1. The compound L^1H (60 mg, 0.23 mmol) was dissolved in 2 mL of water. Two drops of 1 mol dm^{-1} HCl were added, followed by *solid* Mn(ClO$_4$)$_2$·6H$_2$O (80 mg, 0.23 mmol). After 5 min, the solution was filtered. From the filtrate colorless prismatic crystals, suitable for X-ray crystallography, were formed after 2 days. Yield: 20 mg (0.022 mmol, 20%). Anal. Found: C, 36.53; H, 4.00; N, 9.27; Cl, 8.00. Calcd: C, 36.90; H, 4.19; N, 9.22; Cl, 7.78.

$[Mn^{II}_2L^2_2(H_2O)_2](BPh_4)_2 \cdot 2EtOH \cdot 2H_2O$, 2. The compound L^2H (60 mg, 0.22 mmol) was dissolved in 2 mL of water. Solid Mn(NO$_3$)$_2$·6H$_2$O (58 mg, 0.22 mmol) was added. After all solids dissolved, NaBPh$_4$ (70 mg, 0.22 mmol) was added. After 3 h, the white precipitate was collected by filtration. This precipitate was dissolved in EtOH/H$_2$O/MeCN (1/10/2), and pale yellow crystals of **2**, suitable for X-ray crystallography, were formed by slow evaporation of the solvent after 2 days. Yield: 31 mg (0.021 mmol, 19%). Anal. Found: C, 67.68; H, 6.38; N, 5.71. Calcd: C, 67.78; H, 6.38; N, 5.78.

(6) (a) Kessissoglou, D. P.; Kirk, M. L.; Lah, M. S.; Li, X.; Raptopoulou, C.; Hatfield, W. E.; Pecoraro, V. L. *Inorg. Chem.* **1992**, *31*, 5424. (b) Darovsky, A.; Kezerashvili, V.; Coppens, P.; Weyhermueller, T.; Hummel, H.; Weighardt, K. *Inorg. Chem.* **1996**, *35*, 6916. (c) Pal, S.; Olmstead, M. M.; Armstrong, W. H. *Inorg. Chem.* **1995**, *34*, 4708. (d) Oshio, H.; Ino, E.; Mogi, I.; Ito, T. *Inorg. Chem.* **1993**, *32*, 5697. (e) Rardin, R. L.; Poganiuch, P.; Bino, A.; Goldberg, D. P.; Tolman, W. B.; Liu, S.; Lippard, S. J. *J. Am. Chem. Soc.* **1992**, *114*, 5240. (f) Bhula, R.; Weatherburn, D. C. *Angew. Chem., Int. Ed. Engl.* **1991**, *30*, 688. (g) Chen, X.-M.; Tong, Y.-X.; Xu, Z.-T.; Mak, T. C. W. *J. Chem. Soc., Dalton Trans.* **1995**, 4001. (h) Kitajima, N.; Osawa, M.; Tamura, N.; Moro-oka, Y.; Hirano, T.; Hirobe, M.; Nagano, T. *Inorg. Chem.* **1993**, *32*, 1879. (i) Caneschi, A.; Ferraro, F.; Gatteschi, D.; Melandri, M. C.; Rey, P.; Sessoli, R. *Angew. Chem., Int. Ed. Engl.* **1989**, *28*, 1365. (j) Huebner, K.; Roesky, H. W.; Noltemeyer, M.; Bohra, R. *Chem. Ber.* **1991**, *124*, 515. (k) Ménage, S.; Vitols, S. E.; Bergerat, P.; Codjovi, E.; Kahn, O.; Girerd, J.-J.; Guillot, M.; Solans, X.; Calvet, T. *Inorg. Chem.* **1991**, *30*, 2666. (l) Matsushima, H.; Ishiwa, E.; Koikawa, M.; Nakashima, M.; Tokii, T. *Chem. Lett.* **1995**, 129. (m) Reynolds, R. A., III; Yu, W. O.; Dunham, W. R.; Coucouvanis, D. *Inorg. Chem.* **1996**, *35*, 2721. (n) Wu, F.-J.; Kurtz, D. M., Jr.; Hagen, K. S.; Nyman, P. D.; Debrunner, P. G.; Vankai, V. A. *Inorg. Chem.* **1990**, *29*, 5174. (o) Dave, B. C.; Czernuszewicz, R. S.; Bond, M. R.; Carrano, C. J. *Inorg. Chem.* **1993**, *32*, 3593. (p) Corbella, M.; Costa, R.; Ribas, J.; Fries, P. H.; Latour, J.-M.; Öhrström, L.; Solans, X.; Rodrîguez, V. *Inorg. Chem.* **1996**, *35*, 1857. (q) Hulme, C. E.; Watkinson, M.; Haynes, M.; Pritchard, R. G.; McAuliffe, C. A.; Jaiboon, N.; Beagley, B.; Sousa, A.; Bermejo, M. R.; Fondo, M. *J. Chem. Soc., Dalton Trans.* **1997**, 1805.

(7) (a) Mikuriya, M.; Hashimoto, Y.; Kawamori, A. *Chem. Lett.* **1995**, 1095. (b) Pal, S.; Armstrong, W. H. *Inorg. Chem.* **1992**, *31*, 5417. (c) Suzuki, M.; Sugisawa, T.; Senda, H.; Oshio, H.; Uehara, A. *Chem. Lett.* **1989**, 1091. (d) Higuchi, C.; Sakiyama, H.; Okawa, H.; Isobe, R.; Fenton, D. E. *J. Chem. Soc., Dalton Trans.* **1994**, 1097. (e) Gultneh, Y.; Ahvazi, B.; Khan, R.; Butcher, R.; Tuchagues, J. P. *Inorg. Chem.* **1995**, *34*, 3633. (f) Nagata, T.; Mizukami, J. *J. Chem. Soc., Dalton Trans.* **1995**, 2825. (g) Gultneh, Y.; Farooq, A.; Liu, S.; Karlin, K. D.; Zubieta, J. *Inorg. Chem.* **1992**, *31*, 3607. (h) Buchanan, R. M.; Oberhausen, K. J.; Richardson, J. F. *Inorg. Chem.* **1988**, *27*, 971. (i) Downard, A. J.; McKee, V.; Tandon, S. S. *Inorg. Chim. Acta* **1990**, *173*, 181.

(8) (a) Saalfrank, R. W.; Stark, A.; Bremer, M.; Hummel, H.-U. *Angew. Chem., Int. Ed. Engl.* **1990**, *29*, 311. (b) Cano, J.; DeMunno, G.; Sanz, J.; Ruiz, R.; Lloret, F.; Faus, J.; Julve, M. *J. Chem. Soc., Dalton Trans.* **1994**, 3465. (c) Glerup, J.; Goodson, P. A.; Hodgson, D. J.; Michelsen, K. *Inorg. Chem.* **1995**, *34*, 6255.

(9) (a) Bashkin, J. S.; Schake, A. R.; Vincent, J. B.; Chang, H.-R.; Li, Q.; Huffman, J. C.; Christou, G.; Hendrickson, D. N. *J. Chem. Soc., Chem. Commun.* **1988**, 700. (b) Wemple, M. W.; Tsai, H.-L.; Hendrickson, D. N.; Christou, G. *Inorg. Chem.* **1993**, *32*, 2025.

(10) (a) Richards, S.; Pedersen, B.; Silverton, J. B.; Hoard, J. L. *Inorg. Chem.* **1964**, *3*, 27. (b) Nakasuka, N.; Azuma, S.; Katayama, C.; Honda, M.; Tanaka, J.; Tanaka, M. *Acta Crystallogr.* **1985**, *C41*, 1176. (c) Suzuki, M.; Senda, H.; Kobayashi, Y.; Oshio, H.; Uehara, A. *Chem. Lett.* **1988**, 1763. (d) Rockage, S. M.; Sheffer, S. H.; Cacheris, W. P.; Quay, S. C.; Hahn, F. E.; Raymond, K. N. *Inorg. Chem.* **1988**, *27*, 3530. (e) Stilbrany, R. T.; Gorun, S. M. *Angew. Chem., Int. Ed. Engl.* **1990**, *29*, 1156. (f) Inoue, M.; Villegas, C. A.; Asano, K.; Nakamura, M.; Inoue, M.; Fernando, Q. *Inorg. Chem.* **1992**, *31*, 2480. (g) Tanase, T.; Lippard, S. J. *Inorg. Chem.* **1995**, *34*, 4682.

(11) (a) Cox, D. D.; Benkovic, S. J.; Bloom, L. M.; Bradley, F. C.; Nelson, M. J.; Que, L., Jr.; Wallick, D. E. *J. Am. Chem. Soc.* **1988**, *110*, 2026. (b) Cox, D. D.; Que, L., Jr. *J. Am. Chem. Soc.* **1988**, *110*, 8085. (c) Menage, S.; Fujii, H.; Hendrich, M. P.; Que, L., Jr. *Angew. Chem., Int. Ed. Engl.* **1994**, *33*, 1660.

(12) Abufarag, A.; Vahrenkamp, H. *Inorg. Chem.* **1995**, *34*, 2207.

(13) (a) Hazel, A.; Jensen, K. B.; McKenzie, C. J.; Toftlund, H. *J. Chem. Soc., Dalton Trans.* **1993**, 3249. (b) Andersen, U. N.; McKenzie, C. J.; Bojesen, G. *Inorg. Chem.* **1995**, *34*, 1435.

Table 1. Crystallographic Parameters for **1**−**4**

	1	**2**	**3**	**4**
empirical formula	$C_{28}H_{38}N_6O_{17}Cl_2Mn_2$	$C_{82}H_{92}N_6O_{10}B_2Mn_2$	$C_{84}H_{83}N_9O_5B_2Mn_2$	$C_{30}H_{40}N_6O_{18}Cl_2Mn_2$
fw	911.34	1453.16	1430.13	953.46
cryst size (mm)	$0.50 \times 0.50 \times 0.50$	$0.40 \times 0.40 \times 0.40$	$0.20 \times 0.30 \times 0.50$	$0.20 \times 0.20 \times 0.30$
cryst syst	monoclinic	monoclinic	orthorhombic	trigonal
space group	$P2_1/n$	$P2_1/n$	$P2_12_12_1$	$R\bar{3}$
a (Å)	12.19(1)	16.769(2)	27.888(3)	23.962(4)
b (Å)	14.623(8)	9.643(2)	29.054(2)	−
c (Å)	21.72(1)	23.533(2)	9.428(2)	17.190(3)
β (deg)	96.29(6)	92.984(8)	−	−
V (Å^3)	3849(4)	3798.4(7)	7638(2)	8547(3)
D_x (g cm^{-3})	1.417	1.270	1.243	1.482
Z	4	2	4	8
T (K)	293	293	293	293
no. of reflns	5504	6028	7976	3975
no. of obsd reflns ($I > 3\sigma(I)$)	3644	2324	3162	2863
no. of variables	496	460	874	262
μ(Cu Kα) (cm^{-1})	71.67	32.05	31.60	66.45
$F(000)$	1672	1532	3000	3920
scan range (deg)	$1.52 + 0.30 \tan\theta$	$1.42 + 0.30 \tan\theta$	$1.10 + 0.30 \tan\theta$	$1.21 + 0.30 \tan\theta$
$2\theta_{max}$ (deg)	120.2	120.0	140.4	120.0
2θ range of reflns for cell parameter determination (deg)	41−57	46−55	23−45	59−78
max peak (e Å^{-3})	0.74	0.60	0.46	0.91
min peak (e Å^{-3})	−0.89	−0.57	−0.73	−0.57
R^a	0.077	0.068	0.098	0.069
$R_w{}^a$	0.079	0.063	0.101	0.076

^{a} $R = \sum||F_o| - |F_c||/\sum|F_o|$, $R_w = (\sum w(|F_o| - |F_c|)^2/\sum wF_o^2)^{1/2}$ ($w = 1/\sigma^2(F_o^2)$). R and R_w were calculated for observed reflections.

$\{[Mn^{II}{}_2L^2{}_2(H_2O)(MeCN)](BPh_4)_2 \cdot 2MeCN\}_\infty$, **3**. The compound L^{2}H (60 mg, 0.22 mmol) was dissolved in 2 mL of water. Solid Mn-(NO$_3$)$_2$·6H$_2$O (58 mg, 0.22 mmol) was added. After all solids dissolved, NaBPh$_4$ (70 mg, 0.22 mmol) was added. After 3 h, the white precipitate was collected by filtration. This precipitate was recrystallized by vapor diffusion of diethyl ether into an acetonitrile solution. Pale-yellow crystals of **3**, suitable for X-ray crystallography, were formed in 24% yield (38 mg, 0.026 mmol). Anal. Found: C, 70.18; H, 5.75; N, 8.79. Calcd: C, 70.55; H, 5.85; N, 8.81.

[Mn$^{IV}{}_2$O$_2$L$^2{}_2$](ClO$_4$)$_2$·4H$_2$O, 4. To a solution of L^{2}H (60 mg, 0.22 mmol) in 2 mL of water, 2 drops of 1 mol dm^{-1} HCl was added, followed by 58 mg (0.22 mmol) of Mn(NO$_3$)$_2$·6H$_2$O. After 5 min, a few drops of 30% H$_2$O$_2$ were added to the solution until the color turned dark blue. NaClO$_4$ (25 mg, 0.020 mmol) was added. Dark blue crystals of **5**, suitable for X-ray crystallography, were formed after 2 days. Yield: 10 mg (0.011 mmol, 10%). Anal. Found: C, 37.80; H, 4.00; N, 8.91; Cl, 7.47. Calcd: C, 37.80; H, 4.21; N, 8.81; Cl, 7.43.

X-ray Structure Determination. Cell constants and intensity data were collected at 293 K on a Rigaku AFC7R diffractometer equipped with a copper tube (λ(Cu Kα) = 1.541 78 Å) operating at 40 kV 200 mA and a nickel foil filter. The data were corrected for Lorentz−polarization effects. Empirical absorption correction based on a ψ scan was applied except for **2**, for which we could not collect appropriate ψ scan data due to a mechanical problem. Three standard reflections were monitored every 150 reflections; in the case of **3** and **4**, the standard reflections showed −19 and −9% decay, respectively. A linear correction was applied in each case. The structures were solved by direct methods and refined on F by full-matrix least-squares techniques; all calculations were performed by the TEXSAN[14] crystallography software package of Molecular Structure Corporation. Atomic scattering facters were taken from ref 15. All non-hydrogen atoms were refined anisotropically except for the acetonitrile solvate molecules in **3**. Hydrogen atoms were fixed at the calculated positions in **1**, **2**, and **4**; no attempts were made to include hydrogen atoms for **3**. The final R values (calculated for the observed reflections) as well as other crystallographic parameters for **1**−**4**, are listed in Table 1. Unfortunately, all the X-ray structures are of moderate quality, mainly because

of the disordered counteranions (perchlorate and tetraphenylborate) and crystal solvents. Repeated attempts to obtain better crystals and/or better data sets were unsuccessful.

Magnetic Measurement. The magnetic susceptibility measurements of powdered samples were performed by SQUID with Quantum Design model HMPS/HMPS2 in the temperature range 2−300 K. The field strength was 10 000 G in **1**, **2**, and **3**, and 5000 G in **4**. The molar susceptibilities were corrected for ligand diamagnetism by using Pascal's constants.[16] The experimental data were analyzed by nonlinear least-squares calculation performed by Igor Pro (Version 3.03, Wave-Metrics Inc.) running on a Power Macintosh 6300/120.

Electrochemistry. Cyclic voltammetric measurements were performed with a Fuso 321B potentiostat and a Fuso 312B function generator. Acetonitrile was dried according to the literature method.[17] The following conditions were used: supporting electrolyte, 0.1 mol dm^{-3} Et$_4$NClO$_4$ (Nacalai Tesque); working electrode, Pt (0.3 mm diameter); auxiliary electrode, Pt wire; reference electrode, Ag/AgClO$_4$. Ferrocene was used as an internal reference. Approximately 1 mmol dm^{-3} solutions were used.

Results and Discussion

Description of the Structures. [Mn$^{II}{}_2$L$^1{}_2$(H$_2$O)$_4$](ClO$_4$)$_2$·H$_2$O, 1. The selected atomic coordinates, interatomic distances, and bond angles are listed in Tables 2, 3, and 4, respectively. This complex consists of [Mn$^{II}{}_2$L$^1{}_2$(H$_2$O)$_4$]$^{2+}$ cations, perchlorate anions and water molecules. The ORTEP[18] drawing of the cationic core is shown in Figure 1.

Each manganese ion binds to one L^1 ligand to form an "L^1-Mn" fragment (Figure 6). The cationic core is formed by two "L^{1}Mn" fragments, each of which binds to the other fragment through the "bound" carboxylate oxygen atom; the other carboxylate oxygen, the "distant" oxygen, remains uncoordi-

(14) *TEXSAN, Crystal Structure Analysis Package*; Molecular Structure Corporation: The Woodlands, Texas, 1985, 1992.

(15) *International Tables for X-ray Crystallography*; Kynoch Press: Birmingham, England, 1974.

(16) (a) Pascal, P. *Ann. Chim. Phys.* **1910**, *19*, 5. (b) Pacault, A.; Hoarau, J.; Marchand, A. *Adv. Chem. Phys.* **1961**, *3*, 171.

(17) Perrin, D. D.; Armarego, W. L. F. *Purification of Laboratory Chemicals*, 3rd ed.; Pergamon Press: New York, 1988; p 68.

(18) Burnett, M. N.; Johnson, C. K. *ORTEP-III: Oak Ridge Thermal Ellipsoid Plot Program for Crystal Structure Illustrations*; Oak Ridge National Laboratory Report ORNL-6895; Oak Ridge National Laboratory: Oak Ridge, TN, 1996.

Table 2. Selected Atomic Coordinates and Equivalent Isotropic Thermal Parameters (Å^2) for **1**

atom	x	y	z	B_{eq}
Mn(1)	0.6923(1)	0.3628(1)	−0.09272(7)	3.32(8)
Mn(2)	0.7812(1)	0.3811(1)	0.07578(7)	3.09(7)
O(1)	0.6322(5)	0.3825(4)	0.0008(3)	3.2(3)
O(2)	0.4860(6)	0.4157(5)	0.0506(3)	4.4(4)
O(3)	0.8381(5)	0.3608(4)	−0.0210(3)	3.3(3)
O(4)	0.9874(5)	0.4117(5)	−0.0627(3)	4.4(4)
O(5)	0.8221(5)	0.3816(5)	−0.1551(3)	5.2(4)
O(6)	0.7061(5)	0.5245(4)	−0.0783(3)	3.7(3)
O(7)	0.6563(5)	0.4180(5)	0.1387(3)	4.3(4)
O(8)	0.7989(5)	0.5256(4)	0.0466(3)	3.6(3)
N(1)	0.5755(8)	0.4050(7)	−0.1804(4)	4.7(5)
N(2)	0.5151(7)	0.2938(6)	−0.0892(4)	3.7(4)
N(3)	0.7101(8)	0.2068(6)	−0.0953(4)	4.2(5)
N(4)	0.8989(7)	0.4303(6)	0.1596(4)	3.8(4)
N(5)	0.9483(6)	0.2963(6)	0.0805(4)	3.7(4)
N(6)	0.7420(7)	0.2312(6)	0.0870(4)	3.8(4)

**Table 3.** Selected Interatomic Distances (Å) for **1**

Mn(1)−O(1)	2.253(6)	Mn(1)−O(3)	2.233(6)
Mn(1)−O(5)	2.211(7)	Mn(1)−O(6)	2.388(7)
Mn(1)−N(1)	2.333(9)	Mn(1)−N(2)	2.393(8)
Mn(1)−N(3)	2.293(9)	Mn(2)−O(1)	2.303(6)
Mn(2)−O(3)	2.303(6)	Mn(2)−O(7)	2.222(6)
Mn(2)−O(8)	2.223(7)	Mn(2)−N(4)	2.306(8)
Mn(2)−N(5)	2.377(8)	Mn(2)−N(6)	2.261(9)
Mn(1)···Mn(2)	3.712(2)		

Table 4. Selected Bond Angles (deg) for **1**

O(1)−Mn(1)−O(3)	71.6(2)	O(1)−Mn(2)−O(3)	69.5(2)
O(1)−Mn(1)−O(5)	149.6(2)	O(1)−Mn(2)−O(7)	83.8(2)
O(1)−Mn(1)−O(6)	77.3(2)	O(1)−Mn(2)−O(8)	83.3(2)
O(1)−Mn(1)−N(1)	118.2(3)	O(1)−Mn(2)−N(4)	158.4(3)
O(1)−Mn(1)−N(2)	69.0(3)	O(1)−Mn(2)−N(5)	129.9(3)
O(1)−Mn(1)−N(3)	101.0(3)	O(1)−Mn(2)−N(6)	85.7(3)
O(3)−Mn(1)−O(5)	82.0(2)	O(3)−Mn(2)−O(7)	152.6(2)
O(3)−Mn(1)−O(6)	83.2(2)	O(3)−Mn(2)−O(8)	79.3(2)
O(3)−Mn(1)−N(1)	160.3(3)	O(3)−Mn(2)−N(4)	122.5(3)
O(3)−Mn(1)−N(2)	128.7(3)	O(3)−Mn(2)−N(5)	68.3(2)
O(3)−Mn(1)−N(3)	86.2(3)	O(3)−Mn(2)−N(6)	93.5(3)
O(5)−Mn(1)−O(6)	85.0(3)	O(7)−Mn(2)−O(8)	92.2(3)
O(5)−Mn(1)−N(1)	83.2(3)	O(7)−Mn(2)−N(4)	81.2(3)
O(5)−Mn(1)−N(2)	141.4(3)	O(7)−Mn(2)−N(5)	137.9(3)
O(5)−Mn(1)−N(3)	91.8(3)	O(7)−Mn(2)−N(6)	90.1(3)
O(6)−Mn(1)−N(1)	82.7(3)	O(8)−Mn(2)−N(4)	81.8(3)
O(6)−Mn(1)−N(2)	117.7(3)	O(8)−Mn(2)−N(5)	113.5(3)
O(6)−Mn(1)−N(3)	169.3(3)	O(8)−Mn(2)−N(6)	168.5(3)
N(1)−Mn(1)−N(2)	70.4(3)	N(4)−Mn(2)−N(5)	70.9(3)
N(1)−Mn(1)−N(3)	107.1(3)	N(4)−Mn(2)−N(6)	109.8(3)
N(2)−Mn(1)−N(3)	70.7(3)	N(5)−Mn(2)−N(6)	71.4(3)
Mn(1)−O(1)−Mn(2)	109.1(3)	Mn(1)−O(3)−Mn(2)	109.8(3)

nated (see Figure 6 for distinguishing "bound" and "distant" oxygens). Two water molecules bind to each manganese, thereby forming a seven-coordinate structure with an N$_3$O$_4$ donor set. The cation has an approximate C_2 axis passing perpendicular to the average Mn−(O)$_2$−Mn plane.

The Mn−O bond lengths (2.211(7)−2.388(7) Å) are longer than typical Mn^{II}−O bond lengths (2.0−2.2 Å) in octahedral Mn^{II} complexes, which is consistent with the seven-coordinate structure of **1**. For the Mn−N bonds the trend is less prominent; the Mn−N(amine) bonds (2.393(8) and 2.377(8) Å) are longer than in most reported octahedral Mn^{II} complexes (2.25−2.35 Å), whereas the Mn−N(pyridine) bonds (2.261(9)−2.333(9) Å) fall within the range of reported values (2.20−2.38 Å in octahedral Mn^{II} complexes). The reported bond lengths of known seven-coordinate Mn^{II} complexes are 2.11−2.36 Å (Mn−O), 2.21−2.58 Å (Mn−N(amine)), and 2.21−2.42 Å (Mn−N(pyridine)), which match well with the bond lengths in **1**. The bond angles reveal that the geometry of the first
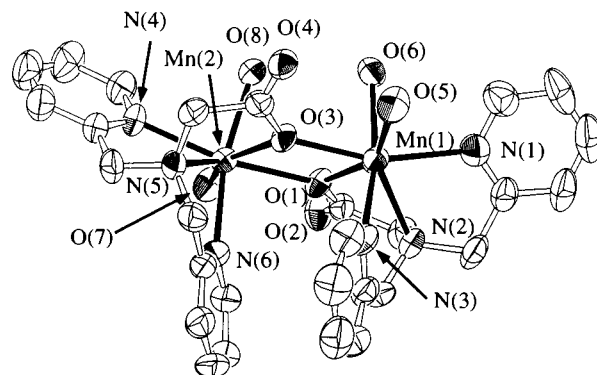
Figure 1. ORTEP view (50% probability thermal ellipsoids) of the [Mn$_2$L$^1_2$(H$_2$O)$_4$]$^{2+}$ cation in **1**.

Table 5. Selected Atomic Coordinates and Equivalent Isotropic Thermal Parameters (Å^2) for **2**

atom	x	y	z	B_{eq}
Mn(1)	0.5291(1)	0.1303(2)	0.05571(8)	4.0(1)
O(1)	0.5698(4)	0.3435(8)	0.0770(3)	5.4(5)
O(2)	0.4979(5)	−0.0992(8)	0.0393(3)	5.3(5)
O(3)	0.5774(6)	−0.251(1)	0.0005(3)	6.4(5)
N(1)	0.5959(6)	0.038(1)	0.1366(4)	4.4(6)
N(2)	0.6573(5)	0.092(1)	0.0341(4)	4.6(6)
N(3)	0.4445(7)	0.147(1)	0.1253(4)	5.0(6)

coordination sphere is quite distorted, unlike some other seven-coordinate Mn^{II} complexes that have pentagonal bipyramidal[19] or monocapped trigonal or antitrigonal prism[20] geometries. However, such distorted seven-coordinate structures are also precedented,[10f] reflecting perhaps the lack of strong structural preference of the d^5 metal ion. Some of the water oxygens (both coordinated and lattice water) are located within 3 Å distances from other oxygen atoms (Table F, Supporting Information). Although these short distances suggest the presence of hydrogen bonding network, we will not discuss the details because of the moderate quality of the X-ray structure. The Mn···Mn distance is 3.712(2) Å.

[Mn$^{II}_2$L$^2_2$(H$_2$O)$_2$](BPh$_4$)$_2$·2EtOH·2H$_2$O, 2. The selected atomic coordinates, interatomic distances, and bond angles are listed in Tables 5, 6, and 7, respectively. This complex consists of dinuclear [Mn^{II}L$^2_2$(H$_2$O)$_2$]$^{2+}$ cations, tetraphenylborate anions, ethanol, and water molecules.

The ORTEP drawing of the dimeric cation (which lies on a crystallographic inversion center) is shown in Figure 2. Two "L^{2}Mn" fragments are linked through the "bound" carboxylate

(19) (a) Drew, M. G. B.; Othman, A. H. B.; McFall, S. G.; McIlroy, P. D. A.; Nelson, S. M. *J. Chem. Soc., Dalton Trans.* **1977**, 438. (b) Drew, M. G. B.; Othman, A. H. B.; McFall, S. G.; McIlroy, P. D. A.; Nelson, S. N. *J. Chem. Soc., Dalton Trans.* **1977**, 1173. (c) Palenik, G. J.; Wester, D. W. *Inorg. Chem.* **1978**, *17*, 864. (d) Pelizzi, C.; Pelizzi, G.; Tarasconi, P. *J. Chem. Soc., Dalton Trans.* **1985**, 215. (e) Capparelli, M. V.; de Meester, P.; Goodgame, D. M. L.; Gunn, S. J.; Skapski, A. C. *Inorg. Chim. Acta* **1985**, *97*, L37. (f) Brooker, S.; McKee, V. *J. Chem. Soc., Dalton Trans.* **1990**, 2397. (g) Bailey, N. A.; Fenton, D. E.; Kitchen, S. J.; Lilley, T. H.; Williams, M. G.; Tasker, P. A.; Leong, A. J.; Lindoy, L. F. *J. Chem. Soc., Dalton Trans.* **1991**, 2989. (h) Brooker, S.; McKee, V. *Acta Crystallogr.* **1993**, *C49*, 441.

(20) (a) Cockman, R. W.; Hoskins, B. F.; McCormick, M. J.; O'Donnell, T. A. *Inorg. Chem.* **1988**, *27*, 2742. (b) Gon, S. G.; You, X.; Yu, K.; Lu, J. *Inorg. Chem.* **1993**, *32*, 1883. (c) Inoue, M. B.; Navarro, R. E.; Inoue, M.; Fernando, Q. *Inorg. Chem.* **1995**, *34*, 6074. (d) Brooker, S.; Kelly, R. J. *J. Chem. Soc., Dalton Trans.* **1996**, 2117. (e) Deroche, A.; Morgenstern-Badaran, I.; Cesario, M.; Gailhem, J.; Keita, B.; Nadjo, L.; Houée-Levin, C. *J. Am. Chem. Soc.* **1996**, *118*, 4567. (f) Mikuriya, M.; Hatano, Y.; Asato, E. *Chem. Lett.* **1996**, 849. (g) Oki, A. R.; Gogineni, P.; Yurchenko, M.; Yound, V. G., Jr. *Inorg. Chim. Acta* **1997**, *257*, 279.

Table 6. Selected Interatomic Distances (Å) for **2**

Mn(1)−O(1)	2.216(7)	Mn(1)−O(2)	2.302(8)
Mn(1)−O(2*)	2.277(8)	Mn(1)−O(3*)	2.461(9)
Mn(1)−N(1)	2.334(9)	Mn(1)−N(2)	2.263(10)
Mn(1)−N(3)	2.227(10)	Mn(1)···Mn(1*)	3.726(4)

Table 7. Selected Bond Angles (deg) for **2**

O(1)−Mn(1)−O(2)	174.1(3)	O(2*)−Mn(1)−O(3*)	55.5(3)
O(1)−Mn(1)−O(2*)	112.8(3)	O(2*)−Mn(1)−N(1)	144.3(4)
O(1)−Mn(1)−O(3*)	83.6(3)	O(2*)−Mn(1)−N(2)	84.3(3)
O(1)−Mn(1)−N(1)	92.4(3)	O(2*)−Mn(1)−N(3)	129.0(4)
O(1)−Mn(1)−N(2)	85.2(3)	O(3*)−Mn(1)−N(1)	157.5(3)
O(2)−Mn(1)−O(2*)	71.1(3)	O(3*)−Mn(1)−N(2)	128.8(3)
O(2)−Mn(1)−O(3*)	102.3(3)	O(3*)−Mn(1)−N(3)	83.6(3)
O(2)−Mn(1)−N(1)	82.2(3)	N(1)−Mn(1)−N(2)	72.6(4)
O(2)−Mn(1)−N(2)	91.0(3)	N(1)−Mn(1)−N(3)	74.1(4)
O(2)−Mn(1)−N(3)	92.6(4)	N(2)−Mn(1)−N(3)	145.6(4)
Mn(1)−O(2)−Mn(1*)	108.9(3)		
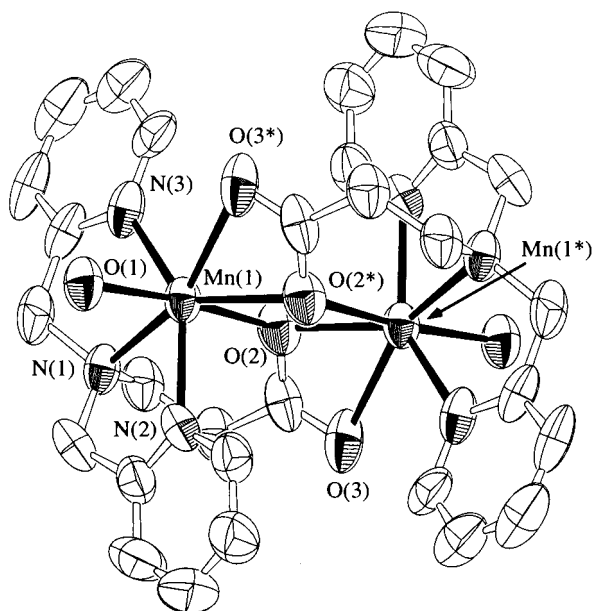
Figure 2. ORTEP view (50% ellipsoids) of the $[Mn_2L^2_2(H_2O)_2]^{2+}$ cation in **2**.

oxygens to form a dimeric structure. Unlike in **1**, the "distant" oxygen in each "L²Mn" fragment coordinates to the manganese ion of the other fragment (see Figure 6 for comparison). The manganese ion is seven-coordinate with an N_3O_4 donor set, namely the four donor atoms from L², the two carboxylate oxygens from the other fragment, and a water molecule. The bond distances show a similar trend as in **1**, and the geometry around each Mn ion is also heavily distorted. The Mn···Mn distance is 3.726(4) Å. There are also short (<3 Å) contacts involving water and ethanol oxygens (Supporting Information, Table L).

$\{[Mn^{II}_2L^2_2(H_2O)(MeCN)](BPh_4)_2 \cdot MeCN\}_\infty$, **3**. The selected atomic coordinates, interatomic distances and bond angles are listed in Tables 8, 9, and 10, respectively. The cationic part of **3** consists of one-dimensional chains, in which manganese ions are bridged by carboxylate groups. These chains extend along the *c* axis. The tetraphenylborate anions and solvate (acetonitrile) molecules are located between these chains. The ORTEP view of the cation chain is shown in Figure 3. The minimum repetition unit of the cationic chain (Figure 4) contains two "L²Mn" fragments. Each fragment is linked to the adjacent one via the "distant" carboxylate oxygen, which results in the μ_2,η^2-bridging mode of the carboxylate group. This is in contrast with the case of **1** and **2**, where the two "L^nMn"

Table 8. Selected Atomic Coordinates and Equivalent Isotropic Thermal Parameters (Å²) for **3**

| atom	x	y	z	B_{eq}
Mn(1)	0.4664(1)	0.1104(1)	0.7375(3)	4.63(7)
Mn(2)	0.5517(1)	0.0855(1)	0.2319(3)	4.10(7)
O(1)	0.4784(4)	0.0960(4)	0.956(1)	6.0(4)
O(2)	0.4893(4)	0.1213(4)	0.172(1)	5.1(3)
O(3)	0.5291(5)	0.0809(4)	0.675(1)	5.6(3)
O(4)	0.5371(4)	0.0983(5)	0.451(1)	6.5(4)
O(5)	0.4493(4)	0.1349(4)	0.509(1)	5.2(3)
N(1)	0.4122(6)	0.0537(5)	0.712(2)	5.6(4)
N(2)	0.3926(5)	0.1395(5)	0.807(2)	4.7(4)
N(3)	0.4813(5)	0.1851(4)	0.784(1)	4.2(4)
N(4)	0.5819(5)	0.0313(5)	0.092(2)	5.1(4)
N(5)	0.6284(5)	0.0694(6)	0.311(2)	5.8(4)
N(6)	0.5943(6)	0.1495(5)	0.199(2)	5.1(4)
N(7)	0.4967(6)	0.0239(6)	0.288(2)	6.9(5)

Table 9. Selected Interatomic Distances (Å) for **3**

Mn(1)−O(1)	2.13(1)	Mn(1)−O(3)	2.03(1)
Mn(1)−O(5)	2.32(1)	Mn(1)−N(1)	2.25(1)
Mn(1)−N(2)	2.32(1)	Mn(1)−N(3)	2.25(1)
Mn(2)−O(2)	2.11(1)	Mn(2)−O(4)	2.14(1)
Mn(2)−N(4)	2.23(1)	Mn(2)−N(5)	2.31(1)
Mn(2)−N(6)	2.23(1)	Mn(2)−N(7)	2.41(2)
Mn(1)···Mn(2)	5.376(4)	Mn(2)···Mn(1*)	5.282(4)

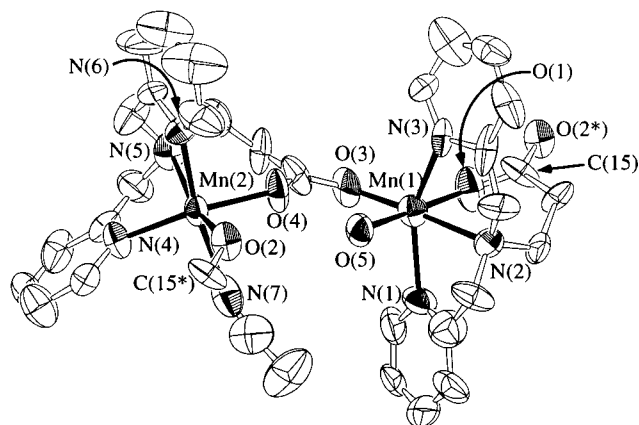**Table 10.** Selected Bond Angles (deg) for **3**

O(1)−Mn(1)−O(3)	93.5(5)	O(2)−Mn(2)−O(4)	91.1(5)
O(1)−Mn(1)−O(5)	172.7(5)	O(2)−Mn(2)−N(4)	120.1(5)
O(1)−Mn(1)−N(1)	93.7(5)	O(2)−Mn(2)−N(5)	162.1(5)
O(1)−Mn(1)−N(2)	86.5(5)	O(2)−Mn(2)−N(6)	89.6(5)
O(1)−Mn(1)−N(3)	88.5(5)	O(2)−Mn(2)−N(7)	84.3(6)
O(3)−Mn(1)−O(5)	92.2(4)	O(4)−Mn(2)−N(4)	140.3(6)
O(3)−Mn(1)−N(1)	103.7(5)	O(4)−Mn(2)−N(5)	84.3(5)
O(3)−Mn(1)−N(2)	176.3(5)	O(4)−Mn(2)−N(6)	95.2(5)
O(3)−Mn(1)−N(3)	107.7(5)	O(4)−Mn(2)−N(7)	78.2(6)
O(5)−Mn(1)−N(1)	89.3(5)	N(4)−Mn(2)−N(6)	72.4(6)
O(5)−Mn(1)−N(2)	88.1(5)	N(4)−Mn(2)−N(6)	107.9(6)
O(5)−Mn(1)−N(3)	85.5(5)	N(4)−Mn(2)−N(7)	81.1(6)
N(1)−Mn(1)−N(2)	72.6(5)	N(5)−Mn(2)−N(6)	73.7(6)
N(1)−Mn(1)−N(3)	148.3(5)	N(5)−Mn(2)−N(7)	111.5(6)
N(2)−Mn(1)−N(3)	76.0(5)	N(6)−Mn(2)−N(7)	170.9(6)

(*n* = 1, 2) fragments are linked via the "bound" oxygens, which results in the μ_2,η^1-bridging mode (see Figure 6 for comparison). Each of the two manganese ions is six-coordinate, namely the four donor atoms from L², the bridging "distant" oxygen, and a water (for Mn(1)) or an acetonitrile (for Mn(2)) molecule. The coordination geometries are significantly distorted from a regular octahedron, as seen from such bond angles as 72.6(5)° (N(1)−Mn(1)−N(2)), 148.3(5)° (N(1)−Mn(1)−N(3)), and 120.1-(5)° (O(2)−Mn(2)−N(4)). The bond lengths are normal except for the longer bonds of the coordinating solvent molecules (Mn-(1)−O(5) = 2.32(1) Å, Mn(2)−N(7) = 2.41(2) Å). The

(21) References 21−26 are classified by the nature of the ligands employed. Bidentate ligands: (a) Plaskin, P. M.; Stoufer, R. C.; Mathew, M.; Palenik, G. J. *J. Am. Chem. Soc.* **1972**, *94*, 2121. (b) Cooper, S, R.; Dismukes, G. C.; Klein, M. P.; Calvin, M. *J. Am. Chem. Soc.* **1978**, *100*, 7248. (c) Stebler, M.; Ludi, A.; Bürgi, H.-B. *Inorg. Chem.* **1986**, *25*, 4743. (d) Libby, E.; Webb, R. J.; Streib, W. E.; Folting, K.; Huffman, J. C.; Hendrickson, D. N.; Christou, G. *Inorg. Chem.* **1989**, *28*, 4037.

(22) Tridentate ligands: (a) Wieghardt, K.; Bossek, U.; Zsolnai, L.; Huttner, G.; Blondin, G.; Girerd, J.-J.; Babonneau, F. *J. Chem. Soc., Chem. Commun.* **1987**, 651. (b) Wieghardt, K.; Bossek, U.; Nuber, B.; Weiss, J.; Bonvoisin, J.; Corbella, M.; Vitols, S. E.; Girerd, J. J. *J. Am. Chem. Soc.* **1988**, *110*, 7398. (c) Bossek, U.; Weyhermüller, T.; Wieghardt, K.; Nuber, B.; Weiss, J. *J. Am. Chem. Soc.* **1990**, *112*, 6387. (d) Niemann, A.; Bossek, U.; Wieghardt, K.; Butzlaff, C.; Trautwein, A. X.; Nuber, B. *Angew. Chem., Int. Ed. Engl.* **1992**, *31*, 311. (e) Pal, S.; Olmstead, M. M.; Armstrong, W. H. *Inorg. Chem.* **1995**, *34*, 4708.
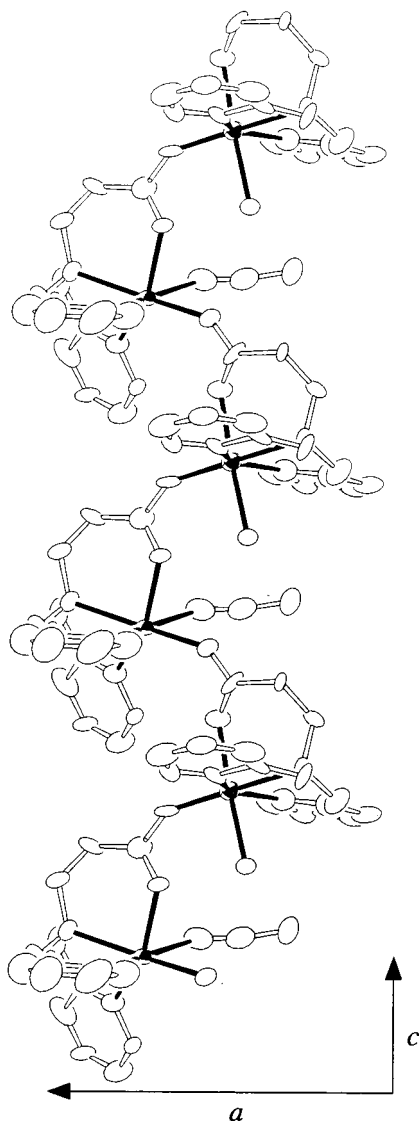
Figure 3. View of the cationic chain $\{[Mn_2L^2_2(H_2O)(MeCN)]^{2+}\}_\infty$ in **3**. The chain runs parallel to the *c* axis.

Table 11. Selected Atomic Coordinates and Equivalent Isotropic Thermal Parameters ($Å^2$) for **4**

atom	x	y	z	B_{eq}
Mn(1)	0.77276(4)	0.14190(5)	0.63733(6)	2.20(2)
O(1)	0.6895(2)	0.1145(2)	0.6803(2)	2.6(1)
O(2)	0.6070(2)	0.1314(2)	0.6899(3)	4.3(1)
O(3)	0.8550(2)	0.1709(2)	0.6033(2)	1.9(1)
N(1)	0.7761(2)	0.2243(2)	0.6105(3)	2.3(1)
N(2)	0.7403(2)	0.1202(2)	0.5257(3)	2.2(1)
N(3)	0.7511(2)	0.0511(2)	0.6345(3)	2.1(1)

Table 12. Selected Interatomic Distances (Å) for **4**

Mn(1)−O(1)	1.910(4)	Mn(1)−O(3)	1.828(4)
Mn(1)−O(3*)	1.787(4)	Mn(1)−N(1)	1.991(5)
Mn(1)−N(2)	2.038(5)	Mn(1)−N(3)	1.968(5)
Mn(1)···Mn(1*)	2.722(2)		

Table 13. Selected Bond Angles (deg) for **4**

O(1)−Mn(1)−O(3)	175.7(2)	O(3)−Mn(1)−N(3)	92.9(2)
O(1)−Mn(1)−O(3*)	93.5(2)	O(3*)−Mn(1)−N(1)	100.2(2)
O(1)−Mn(1)−N(1)	86.9(2)	O(3*)−Mn(1)−N(2)	172.0(2)
O(1)−Mn(1)−N(2)	94.4(2)	O(3*)−Mn(1)−N(3)	98.0(2)
O(1)−Mn(1)−N(3)	88.7(2)	N(1)−Mn(1)−N(2)	81.8(2)
O(3)−Mn(1)−O(3*)	82.3(2)	N(1)−Mn(1)−N(3)	161.5(2)
O(3)−Mn(1)−N(1)	92.8(2)	N(2)−Mn(1)−N(3)	80.7(2)
O(3)−Mn(1)−N(2)	89.8(2)	Mn(1)−O(3)−Mn(1*)	97.7(2)

Figure 4. ORTEP view (50% ellipsoids) of the $[Mn_2L^2_2(H_2O)\text{-}(MeCN)]^{2+}$ repetition unit in **3**. The atoms O(2) and C(15) appear twice to show how the adjacent units are connected.

separations between the two manganese centers are 5.376(4) and 5.282(4) Å, which are much longer than those in **1** and **2**.

$[Mn^{IV}_2O_2L^2_2](ClO_4)_2\cdot4H_2O$, 4. The selected atomic coordinates, interatomic distances, and bond angles are listed in Tables 11, 12, and 13, respectively. The ORTEP drawing of

Figure 5. ORTEP view (50% ellipsoids) of the $[Mn_2L^2_2O_2]^{2+}$ cation in **4**.

the cation is shown in Figure 5. The cation lies on the crystallographic inversion center, and has an Mn−(μ-O)$_2$−Mn core which is very common in Mn^{III} and Mn^{IV} complexes.[10c,21−26] Unlike **1**−**3**, the carboxylate oxygen atoms do not bridge the manganese atoms, although the dimeric cation in **4** also contains two "L^{2}Mn" fragments. Each manganese ion has a six-coordinate, octahedral geometry with no evidence of Jahn−Teller elongation; this observation, as well as the charge balance, supports the "Mn^{IV}$_2$" formulation for this complex. The bond lengths are within the range observed for other Mn^{IV} complexes. The magnetic and electrochemical properties were also consistent with this formulation (see below).

(23) Tetradentate ligands, aliphatic amines: (a) Hagen, K. S.; Armstrong, W. H.; Hope, H. *Inorg. Chem.* **1988**, *27*, 967. (b) Brewer, K. J.; Calvin, M.; Lumpkin, R. S.; Otvos, J. W.; Spreer, L. O. *Inorg. Chem.* **1989**, *28*, 4446. (c) Goodson, P. A.; Hodgson, D. J.; Michelson, K. *Inorg. Chim. Acta* **1990**, *172*, 49.
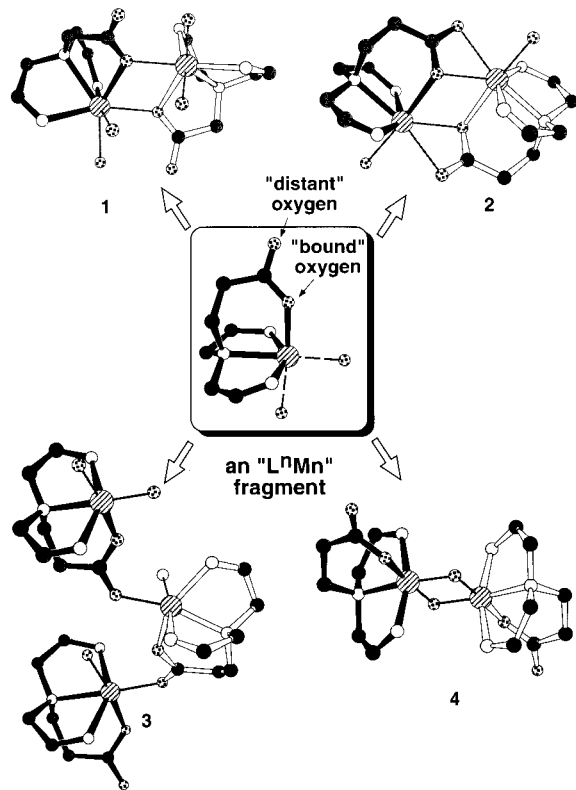
Figure 6. Schematic view showing how the "L^{n}Mn fragments" are connected in the structures of **1**−**4**. Each dimeric unit is composed from two fragments, one is shown in black bonds and the other in white bonds. The gray thin bonds represent interfragment bonds and bonds to additional ligands (e.g. H$_2$O). The carbon atoms of the pyridine rings and the hydrogen atoms are omitted for clarity.

Structural Variation in Complexes 1−4. The ligands L^1 and L^2 form three structurally different types of manganese complexes; bis(μ-carboxylato) Mn^{II} dimers (**1** and **2**), a carboxylato-bridged Mn^{II} polymer (**3**), and bis(μ-oxo) Mn^{III}/Mn^{IV} dimers (**4** and Suzuki's complex, [Mn^{III}Mn^{IV}O$_2$L^1$_2$](ClO$_4$)^{10c}). These structures share a common structural motif, an "L^{n}Mn fragment", in which an Mn ion is cheleted by one L^n ligand (Figure 6). The three different structural types found in **1−4** are ascribed to different modes of concatenation of L^{n}Mn fragments, that is, which atom(s) in one fragment binds to the

(24) Tetradentate ligands, aromatic amines: (a) Collins, M. A.; Hodgson, D. J.; Michelsen, K.; Towle, D. K. *J. Chem. Soc. Chem. Commun.* **1987**, 1659. (b) Suzuki, M.; Tokura, S.; Suhara, M.; Uehara, A. *Chem. Lett.* **1988**, 477. (c) Towle, D. K.; Botsford, C. A.; Hodgson, D. J. *Inorg. Chim. Acta* **1988**, *141*, 167. (d) Goodson, P. A.; Hodgson, D. J. *Inorg. Chem.* **1989**, *28*, 3606. (e) Goodson, P. A.; Oki, A. R.; Glerup, J.; Hodgson, D. J. *J. Am. Chem. Soc.* **1990**, *112*, 6248. (f) Oki, A, R.; Glerup, J.; Hodgson, D. J. *Inorg. Chem.* **1990**, *29*, 2435. (g) Goodson, P. A.; Glerup, J.; Hodgson, D. J.; Michelsen, K.; Pedersen, E. *Inorg. Chem.* **1990**, *29*, 503. (h) Goodson, P. A.; Glerup, J.; Hodgson, D. J.; Michelsen, K.; Weihe, H. *Inorg. Chem.* **1991**, *30*, 4909. (i) Frapart, Y.-M.; Boussac, A.; Albach, R.; Anxolabéhère-Mallart, E.; Delroisse, M.; Verlhac, J.-B.; Blondin, G.; Girerd, J.-J.; Guilhem, J.; Cesario, M.; Rutherford, A. W.; Lexa, D. *J. Am. Chem. Soc.* **1996**, *118*, 2669.
(25) Schiff-base ligands: (a) Miller, J. D.; Oliver, D. *J. Inorg. Nucl. Chem.* **1972**, *34*, 1873. (b) Maslen, H. S.; Waters, T. N. *J. Chem. Soc. Chem. Commun.* **1973**, 760. (c) McAuliffe, C. A.; Parish, R. V.; Abu-El-Wafa, S. M.; Issa, R. M. *Inorg. Chim. Acta* **1986**, *115*, 91. (d) Larson, E. J.; Pecoraro, V. L. *J. Am. Chem. Soc.* **1991**, *113*, 3810. (e) Gohdes, J. W.; Armstrong, W. H. *Inorg. Chem.* **1992**, *31*, 368. (f) Larson, E.; Lah, M. S.; Li, X.; Bonadies, J. A.; Pecoraro, V. L. *Inorg. Chem.* **1992**, *31*, 373. (g) Dailey, G. C.; Horwitz, C. P.; Lisek, C. A. *Inorg. Chem.* **1992**, *31*, 5325. (h) Torayama, H.; Nishide, T.; Asada, H.; Fujiwara, M.; Matsushita, T. *Chem. Lett.* **1996**, 387.
(26) Hexadentate ligands: Pal, S.; Gohdes, J. W.; Wilisch, W. C. A.; Armstrong, W. H. *Inorg. Chem.* **1992**, *31*, 713.
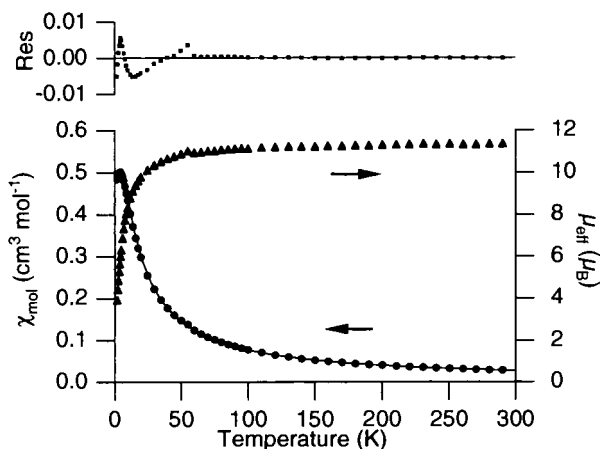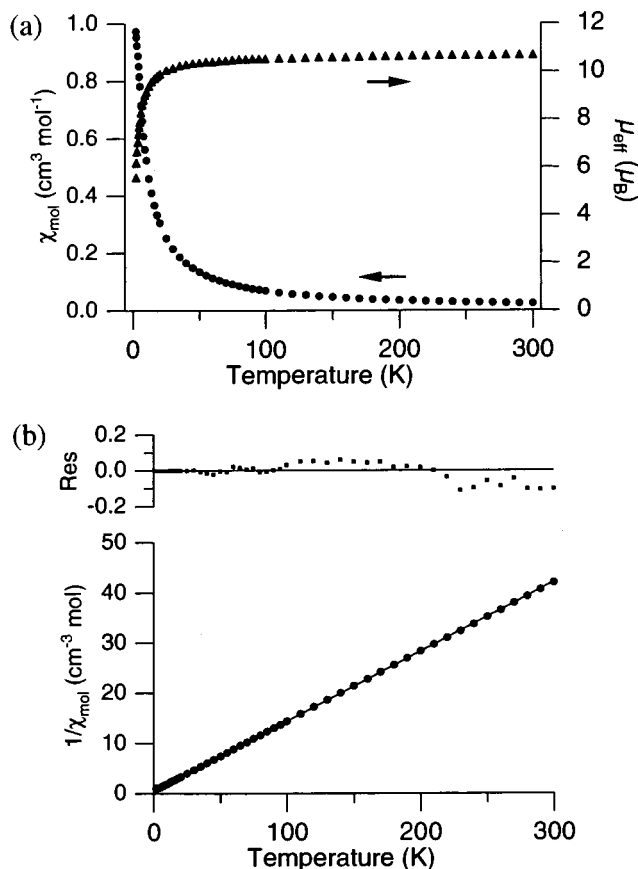

Figure 7. (Bottom) Molar magnetic susceptibility χ_{mol} (cgs units) and the effective magnetic moment μ_{eff} (per one dimeric unit) of **1**. (Top) Difference between the measured and calculated susceptibility.
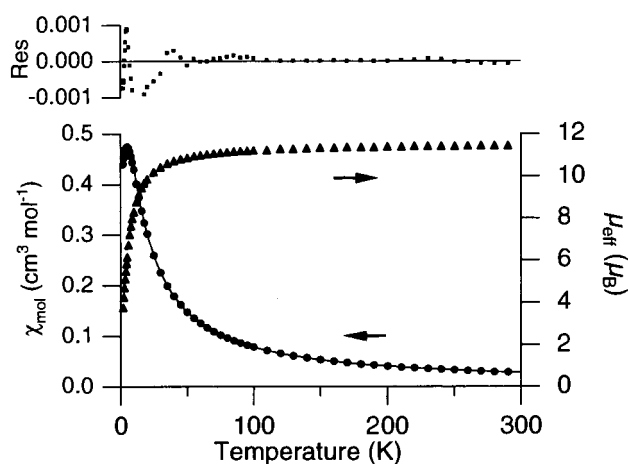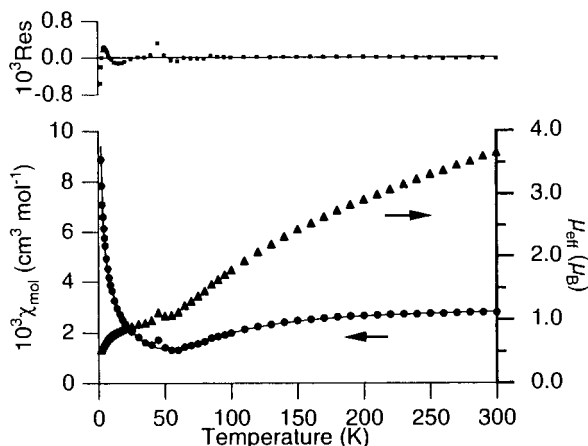

Figure 8. (Bottom) Molar magnetic susceptibility χ_{mol} (cgs units) and the effective magnetic moment μ_{eff} (per one dimeric unit) of **2**. (Top) Difference between the measured and calculated susceptibility.

Mn atom in another fragment. In complexes **1** and **2**, the "bound oxygen" serves as the interfragment bridge; in complex **3**, the "distant oxygen" serves as the bridge whereas the "bound oxygen" does not; in complex **4** and Suzuki's complex, the bridging atoms are not from L^{n}Mn fragments but from the two μ-oxo ligands.

We mentioned in the introduction that the chelating carboxylate ligands would be potentially useful in controlling the structures of manganese−carboxylate clusters. In this context, we would like to point out two advantages of the ligands L^1 and L^2. First, the "bound oxygen" in the L^{n}Mn fragment binds to the Mn atom in an anti mode exclusively, which leads to a relatively rare bis(μ_2,η^1-carboxylato) structure in **1** and **2**, and a *syn,anti*-(μ_2,η^2-carboxylato) structure in **3**. Second, we can assume the L^{n}Mn fragment as a building block of the crystal structure and can focus on the site and geometry of interfragment connections, which simplifies the task to design the target structure(s). On the other hand, formation of **2** and **3** under very similar conditions (the recrystallization solvent was the only difference) indicates that L^1 and L^2 were still too simple to control the structure effectively. We will continue to seek better ligands that will give us better control of the formation of manganese complexes. (Please note that Figure 6 is just a schematic representation of the structures reported here, rather than a suggestion for the mechanism of formation of such structures. However, it may be interesting to take Figure 6 as

Figure 9. (a) Molar magnetic susceptibility χ_{mol} (cgs units) and the effective magnetic moment μ_{eff} (per one dimeric unit) of **3**. (b) Curie–Weiss plot (i.e. $1/\chi_{mol}$ vs T) for **3**. The residues are shown on the top part.

Figure 10. (Bottom) Molar magnetic susceptibility χ_{mol} (cgs units) and the effective magnetic moment μ_{eff} (per one dimeric unit) of **4**. (Top) Difference between the measured and calculated susceptibility.

a basis of working hypothesis for studying the solution chemistry of these compounds, although we are not currently planning in-depth studies of such kind.) Finally, L^1 and L^2 are the first polydentate chelating ligands with carboxylate groups which gave manganese complexes of different oxidation states. We can expect that other manganese complexes of carboxylate-containing chelates[10] may also reveal interesting structural diversity at different oxidation levels.

Magnetic Susceptibility. The magnetic susceptibilities of **1**–**4** were measured in the range 2–300 K (Figures 7–10; all χ_{mol} data are given in cgs units). For the two binuclear Mn^{II}

complxes (**1** and **2**), the temperature dependence of μ_{eff} was similar; at room temperature the effective magnetic moment per 1 mol of dinuclear unit was 11.4 μ_B (close to the calculated spin-only value of 11.8 μ_B for two independent high-spin d^5 ions; μ_B is the Bohr magneton), and decreased monotonically as the temperature was lowered. The magnetic susceptibility (χ_{mol}) showed a maximum at 4.5–5.0 K, the typical behavior for a weakly antiferromagnetic coupling. We analyzed the χ_{mol} data by fitting to the eq 1 derived from the isotropic Heisenberg exchange Hamiltonian $H = -2JS_1 \cdot S_2$:

$$\chi_{mol} = \frac{Ng^2\beta^2}{3kT} \frac{\sum_{S_T} S_T(S_T + 1)(2S_T + 1)\exp(JS_T(S_T + 1)/kT)}{\sum_{S_T}(2S_T + 1)\exp(JS_T(S_T + 1)/kT)} + K + \frac{C}{T} \tag{1}$$

where S_T (the total spin quantum number) assumes the values of 0, 1, 2, 3, 4, and 5 for the $S_1 = S_2 = \frac{5}{2}$ (i.e. two high-spin d^5 ions) system; g is Landé's g factor, J is the exchange integral, K accounts for TIP (temperature-independent paramagnetism) and a small correction to the diamagnetic contribution, and C/T accounts for the paramagnetic impurities; N, β, and k are Avogadro's number, the Bohr magneton, and Boltzmann's constant, respectively. Good-fitting curves were obtained for the following parameters: complex **1**, $J = -0.631(6)$ cm^{-1}, $g = 1.912(4)$, $K = 3(2) \times 10^{-4}$ cm^3 mol^{-1}, $C = 0.13(1)$ cm^3 K mol^{-1} (corresponding to 3.0(3)% of monomeric Mn^{II} impurities); complex **2**, $J = -0.655(5)$ cm^{-1}, $g = 1.941(3)$, $K = 2(1) \times 10^{-4}$ cm^3 mol^{-1}, $C = 0.04(1)$ cm^3 K mol^{-1} (1.0(3)% of Mn^{II} impurities).

The effective magnetic moment of **3** (Figure 9, part a) was 10.6 μ_B at room temperature and also declined monotonically with decreasing temperature. Unlike the cases of **1** and **2**, χ_{mol} continued to increase as the temperature approached our lower limit (2.0 K). To estimate the magnetic coupling between the adjacent Mn ions, we employed a Curie–Weiss treatment and a molecular field approximation.[27,28] The $1/\chi_{mol}$ vs T plot in the range 30–300 K gave a straight line (Figure 9, part b) which gave a Weiss constant $\Theta = -3.4(2)$ K (where $1/\chi_{mol} = (T - \Theta)/C$). The molecular field theory gives $\Theta = 2zJS(S + 1)/3k$,[29] where z is the number of interacting magnetic ions, and assuming $z = 2$ (because **3** is a linear chain of Mn ions) and $S = \frac{5}{2}$ (high-spin d^5 ion), we obtained $J = -0.20(1)$ cm^{-1}.

The J values of the complexes **1**–**3**, as well as those of the reported Mn^{II} complexes with bridging carboxylates, are compiled in Table 14. In all complexes, the J values are small and negative, which indicates weak antiferromagnetic coupling in these complexes. The doubly bridged complexes **1** and **2** showed larger magnetic coupling than the singly bridged complex **3**. From Table 14, we can see that the $|J|$ values tend to increase as increasing the number of the bridging ligands,
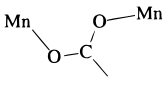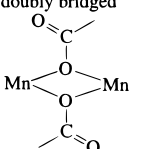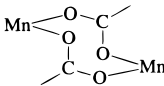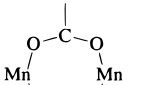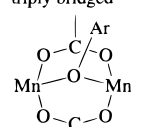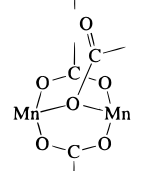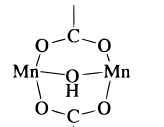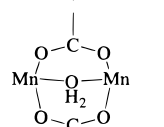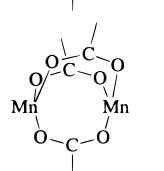
(27) Smart, J. S. *Effective Field Theories of Magnetism*; W. B. Saunders Co.: Philadelphia, 1966.

(28) Since the structure of **3** contains two independent manganese ions, there are two structurally different Mn–Mn pairs, namely Mn(1)–Mn(2) and Mn(2)–Mn(1*). We assume here that the exchange integrals for these two pairs are identical. This would be a good approximation for the simple calculation employed here, because the Mn–Mn distances are similar (5.376(4) and 5.282(4) Å).

(29) For this equation to be valid, the temperature should be high enough to give $g\mu_B SH/kT \ll 1$.[27] This requirement is fulfilled for $T > 30$ K.

Table 14. Mn−Mn Distances and Magnetic Coupling in Carboxylate-Bridged Mn^{II} Complexes

bridging mode	Mn–Mn distance (Å)	J (cm^{-1})	ref
singly bridged			
	5.598(3)	−0.193	6g
	5.40	−0.30(1)	5f
	5.376(4), 5.282(4)	−0.20(1)	this work
doubly bridged			
	3.712(2)	−0.631(6)	this work
	3.726(4)	−0.655(5)	this work
	4.145(1)	−0.972(6)	6d
	4.643(1)	−1.35	8b
	5.626(4)	−1.91	8c
	5.610(1)	−2.04	
triply bridged			
	3.337(2)–3.344(2)	−2.5	30a
	3.325(3)	−4.0	30b
	3.376(2)	−3.2	7d
	3.370(3)–3.716(2)	−4.8(6)	6e
	3.614(1)	−4.4	6k
	3.498(4)	−1.1	6l
	3.351(3)	−9(1)	30c
	3.5950(9)	−2.73(2)	30d
	3.621(2)	−2.952(7)	30d
	3.739(2)	−3.3(2)	6i
	4.034(2)	−3.5	30e
	3.688(8)	−0.2	6l

although there are a few exceptions (i.e. the two complexes reported by Koikawa[6l]). It is worth noting that the complexes **1** and **2** showed the weakest coupling among the doubly bridged complexes, despite the smallest Mn−Mn distances. This suggests that the superexchange mechanism is operating in these complexes and that the μ_2,η^1-carboxylato (i.e. monatomic) bridges in **1** and **2** are less capable of transmitting magnetic

interaction than the μ_2,η^2-carboxylato bridges in other doubly bridged complexes in Table 14.

The $\mu_{eff}-T$ curve of complex **4** looks like a superposition of two components (Figure 10). At higher temperature ($T > 50$ K), μ_{eff} declines gradually with decreasing temperature (3.66 μ_B at 300 K to 1.06 μ_B at 50 K), which is a typical behavior of a strongly antiferromagnetic couple. On the other hand, there is a sudden decrease below 20 K (0.86 μ_B at 20 K to 0.54 μ_B at 2 K), which is characteristic of a weakly antiferromagnetic couple. Attempts to fit the χ_{mol} data of **4** with eq 1 were not successful. Therefore, we tried to fit χ_{mol} to a sum of two "dimeric" components, plus a TIP constant K and a Curie term C/T, as in eq 2:

$$\chi_{mol} = \frac{N\beta^2}{3kT} \times$$

$$\left\{ (1-p)g_A^2 \frac{\displaystyle\sum_{S_T=|S_1-S_2|}^{S_1+S_2} S_T(S_T+1)(2S_T+1)\exp(J_A S_T(S_T+1)/kT)}{\displaystyle\sum_{S_T=|S_1-S_2|}^{S_1+S_2}(2S_T+1)\exp(J_A S_T(S_T+1)/kT)} + \right.$$

$$\left. pg_B^2 \frac{\displaystyle\sum_{S'_T=|S'_1-S'_2|}^{S'_1+S'_2} S'_T(S'_T+1)(2S'_T+1)\exp(J_B S'_T(S'_T+1)/kT)}{\displaystyle\sum_{S'_T=|S'_1-S'_2|}^{S'_1+S'_2}(2S'_T+1)\exp(J_B S'_T(S'_T+1)/kT)} \right\} +$$

$$K + \frac{C}{T} \quad (2)$$

where the spin states of the two dimeric components are assumed to be (S_1, S_2) and (S'_1, S'_2), respectively, and p is the molar ratio of the second component. To reduce the number of parameters, we fixed K as 0, and introduced two variables $g' = (1-p)^{1/2}g_A$ and $p' = pg_B^2$. After obtaining g' and p' by least-squares calculation, we made an assumption $g_B = 2$ (which is a good approximation for most manganese complexes) to obtain p and g_A. The spin state of the first (principal) component was fixed as $(S_1, S_2) = (^3/_2, ^3/_2)$, that is, an Mn$^{IV}_2$ dimer. Trials with $(S_1, S_2) = (2, ^3/_2)$ (an Mn^{III}Mn^{IV} dimer) did not give acceptable fits; trials with $(S_1, S_2) = (2, 2)$ (an Mn$^{III}_2$ dimer) did give reasonable fits, but this formulation was rejected because it was not consistent with the X-ray results (i.e. the presence of two perchlorate anions per dimeric unit and no Jahn−Teller distortion). The second (minor) component can be one of the following: Mn$^{II}_2$, Mn^{II}Mn^{III}, Mn$^{III}_2$, or Mn^{III}Mn^{IV}. We carried out calculation for each one of these four possibilities, and all resulted in similar J_A, g_A, and p values (Supporting Information, Table V and Figure A). Figure 10 shows the results with the formulation "Mn$^{IV}_2$ (principal) with a minor amount of Mn$^{II}_2$" assumed. This calculation gave $J_A = -97.5$-(5) cm^{-1} and $g_A = 1.871(6)$ for the principal (99.4%) Mn$^{IV}_2$ component, and $J_B = -0.84(2)$ cm^{-1} for the minor (0.6%) "Mn$^{II}_2$" component.

Table 15 shows the J values and structural parameters of **4** and other reported Mn$^{IV}_2(\mu$-O)$_2$ complexes (with no other bridging ligands). As Hodgson et al. have pointed out,[24f,h] correlation between the bridging structures and J values is not obvious. We notice, however, that the J values tend to be smaller when the ligand (other than the bridging oxo) carries oxygen donor atoms (see the last three rows). Further experi-

Table 15. Comparison of the Magnetic Coupling Constant J and Structural Parameters for $Mn^{IV}_2(\mu\text{-}O)_2$ Complexes

compound[a]	$-J$ (cm^{-1})	Mn···Mn (Å)	Mn–O–Mn (deg)	ref
$[Mn_2(bpea)_2Cl_2(\mu\text{-}O)_2]^{2+}$	147	2.757	99.2	22e
$[Mn_2(phen)_4(\mu\text{-}O)_2]^{4+}$	144	2.748	99.5	21c
$[Mn_2(L3)_2(\mu\text{-}O)_2]^{4+}$	131	2.747	101.5	24f
$[Mn_2(bispicen)_2(\mu\text{-}O)_2]^{4+}$	126	2.672	95.0, 95.2	24g
$[Mn_2(bispictn)_2(\mu\text{-}O)_2]^{4+}$	106	2.719	98.4, 97.3	24h
$[Mn_2L^2_2(\mu\text{-}O)_2]^{2+}$	98	2.722	97.7	this work
$Mn_2(pic)_4(\mu\text{-}O)_2$	87	2.747	98.1	21d
$Mn_2(salpn)_2(\mu\text{-}O)_2$	82	2.728	97.2	25e

[a] Abbreviations: bpea = *N,N*-bis(2-pyridylmethyl)ethylamine, phen = 1,10-phenanthroline, L3 = (2-(2-pyridyl)ethyl)(6-methyl-2-pyridylmethyl)(2-pyridylmethyl)amine, bispicen = *N,N'*-bis(2-pyridylmethyl)-1,2-ethylenediamine, bispictn = *N,N'*-bis(2-pyridylmethyl)-1,3-propanediamine, picH = pyridine-2-carboxylic acid, salpnH$_2$ = 1,3-bis(salicylideneamino)propane.

mental and theoretical study will be needed to establish this observation as a rule.

Electrochemical Properties. Cyclic voltammograms of the Mn^{II}_2 complexes **1** and **2** in acetonitrile showed irreversible oxidation waves. On the other hand, the Mn^{IV}_2 complex **4** in acetonitrile exhibited two reversible waves with $E_{1/2}$ values of -0.52 and 0.28 V (vs ferrocene), which were assigned to the $Mn^{III}_2/Mn^{III}Mn^{IV}$ and $Mn^{III}Mn^{IV}/Mn^{IV}_2$ redox couples, respectively. These $E_{1/2}$ values are more negative by 0.1 V than those of Suzuki's closely related complex $[Mn^{III}Mn^{IV}O_2L^1_2](ClO_4)$ $(-0.41$ and 0.37 V),[10c] which has the same set of the donor atoms with one intervening CH$_2$ group missing. A similar change was observed by Hodgson et al. in the manganese complexes of tris(2-pyridylmethyl)amine analogues, where adding one extra CH$_2$ group caused a negative shift by 0.05 V.[24f] This $E_{1/2}$ shift is also consistent with the fact that we isolated **4** as an Mn^{IV}_2 dimer whereas Suzuki et al. isolated their compound as an $Mn^{III}Mn^{IV}$ dimer under very similar conditions. Although we do not yet understand how the chain length between the donor groups affects the oxidation potentials, these observation may offer a useful method to control oxidation potentials of the complexes while using a given set of donor groups.

Interestingly, the resting potential of 0.28 V (vs ferrocene) was recorded for a 1 mM solution of **4** in CH$_3$CN/0.1 M Et$_4$-NBF$_4$. This is the same value as $E_{1/2}$ for the $Mn^{III}Mn^{IV}/Mn^{IV}_2$ couple, which suggests that approximately half of **4** was reduced to the $Mn^{III}Mn^{IV}$ state upon dissolving in CH$_3$CN. Consistent with this observation was the multiline EPR spectrum[31] of **4** in *N*-methylformamide glass at 4.2 K (Supporting Information, Figure B), which resembles the reported spectra for various $Mn^{III}Mn^{IV}$ complexes.[21b,22a,23b,c,24b,f−i] It follows that, although **4** is obtained as an Mn^{IV}_2 complex from an aqueous solution, it is highly oxidizing and easily reduced in organic solvents. Such a reaction may be of interest, because hydrogen abstraction by several $Mn(\mu\text{-}O)_2Mn$ complexes has been studied[32] and related to water oxidation in green plant photosynthesis.[33]

(30) (a) Mikuriya, M.; Fujii, T.; Kamisawa, S.; Kawasaki, Y.; Tokii, T.; Oshio, H. *Chem. Lett.* **1990**, 1181. (b) Sakiyama, H.; Tamaki, H.; Kodera, M.; Matsumoto, N.; Okawa, H. *J. Chem. Soc., Dalton Trans.* **1993**, 591. (c) Bossek, U.; Wieghardt, K.; Nuber, B.; Weiss, J. *Inorg. Chim. Acta* **1989**, *165*, 123. (d) Yu, S.-B.; Lippard, S. J.; Shweky, I.; Bino, A. *Inorg. Chem.* **1992**, *31*, 3502. (e) Wieghardt, K.; Bossek, U.; Nuber, B.; Weiss, J.; Bonvoisin, J.; Corbella, M.; Vitols, S. E.; Girerd, J. J. *J. Am. Chem. Soc.* **1988**, *110*, 7398.
(31) We are grateful to one of the reviewers for advising us to obtain an EPR spectrum of **4**.
(32) Wang, K.; Mayer, J. M. *J. Am. Chem. Soc.* **1997**, *119*, 1470.
(33) Baldwin, M. J.; Pecoraro, V. L. *J. Am. Chem. Soc.* **1996**, *118*, 11325.